Indian Journal of Pure & Applied Physics
Vol. 56, December 2018, pp. 949-958

Design of log domain differential class AB universal biquad filter by employing lossy integrators

Niyazi Duduk[a]* & Abdullah T Tola[b]

[a]Department of Electronics and Automation, Denizli Vocational School of Technical Sciences, Pamukkale University, 20160 Kinikli, Denizli, Turkey

[b]Department of Electrical-Electronics Engineering, Faculty of Engineering, Pamukkale University, 20160 Kinikli, Denizli, Turkey

Received 7 January 2018; accepted 18 June 2018

A new current mode low voltage differential Class AB second order universal biquad filter has been designed in this work. In design process, inspiring from Kerwin-Huelsman-Newcomb circuit, the circuit is realized with lossy integrators. The circuit has fundamental filter outputs namely; low pass, high pass and band pass. All pass and notch filter outputs have also been obtained by using additional circuits. In circuit design process, the state space method and translinear principle have been used. Two of the circuit parameters are electronically tunable which are the quality factor Q and the pole frequency f_0. PSpice circuit simulations have been obtained to check the theoretical results' validity. In PSpice simulations, both ideal and AT&T CBIC-R type real transistor models have been used.

Keywords: Active filters, Bipolar transistor circuits, Current-mode circuits, Differential Class AB

1. Introduction

The KHN (Kerwin-Huelsman-Newcomb) biquad has some characteristics that provide some advantages to designers which are low sensitivity, low component spread and good stability[1,2]. Two lossless integrators including feedback loops and a summer block are found in a KHN block. Fundamental filter outputs which are low pass, high pass and band pass filters are obtained, moreover all pass and notch filter outputs can be obtained by additional summer blocks from a KHN circuit. In the literature, there are many KHN filter circuits designed by voltage mode or current mode realization methods[3-12].

Current-mode circuits have better characteristics than voltage-mode circuits, e.g., higher linearity, less power consumption and wider bandwidth[8]. After a general state space synthesis method for log domain filter synthesis was developed by Frey[13,14], this subject became popular. If one wants to design continuous time active filter, log domain filters are good alternatives that they have good characteristics such as low voltage, low power consumption, high linearity and electronical tunability[15,16]. Log domain filters are the members of externally linear internally nonlinear (ELIN) circuits[17]. Log domain circuits are designed by using the translinear circuit structure, so the signal processing operations in log domain circuits are nonlinear, however the transfer function is linear[13,17].

Companding idea is used in log domain filters[18,19]. By using a bipolar transistor, the input current is compressed by a logarithmic function. A bipolar transistor's emitter-base voltage is logarithm of the current of the device. By applying the signal to a bipolar transistor's base-emitter junction, the output voltage is expanded. The output current is exponential of the output voltage. Output function is the reverse function of the input function so the transfer function is linear. Companding offers wide dynamic range[19].

One of the circuit classifications for output stages of amplifiers is based on the bias currents of the output transistors, which is Class A, Class B, or Class AB. This type of circuit classification became also applicable for filter circuits after filtering in the log domain idea had been proposed. Class A type circuit means that all active devices are running in active region, typically transistors that their bias point is set to a value which is greater than the largest expected signal amplitude. This type of circuits achieves high linearity and wide bandwidth but their power consumption is high and dynamic range is narrow. The quiescent currents are set to zero in Class B type circuit designs. There are pairs of output circuits, each conduct for only half cycle of the input signal. Half of the circuit processes positive input signals while the

*Corresponding author (E-mail: nduduk@pau.edu.tr)

other half is cutoff, for negative input signals the opposite situation occurs. This type of operation decreases the power consumption and constant noise but during the transition across positive and negative part of the input signal, the circuit generates disadvantageous crossover distortion. By combining the two types of circuit types, differential Class AB type was introduced. In this type of circuit, all active devices' bias point is set to a value which is much smaller than the largest expected signal amplitude. Differential Class AB type operation takes the advantages of both Class A and Class B circuit structures. For small signals it has the quality of a Class A circuit and for large signals it has efficiency of a Class B circuit. Therefore, it results a circuit has low distortion, low power consumption and low noise characteristics[20].

This work aims to use the good characteristics of the KHN filter block, log-domain and companding idea mentioned above. The most important difference of the designed filter from classical KHN structure is using lossy integrators, not integrators.

The proposed filter in this paper is realized by using differential Class AB type circuit. This work is developed version of our previous work which is Class A type[21]. In the literature, there are some works about Class A and differential Class AB log domain filter circuits[22,23].

In this study, in short, a new current mode log domain differential Class AB universal filter inspired from KHN structure is designed by the state-space synthesis method.

2. State-Space Synthesis Method

State-space method is an efficient approach for realization of a filter transfer function. This method is suitable for nonlinear system design such as log domain filter design[13,15].

First order differential equations and an output equation maintain the state-space representation of a system. A circuit can have more than one state space representation but a state space representation has only one transfer function. A few circuits can be synthesized by using different methods or different elements from same equations. This is the advantage of the state-space method.

The following state-space equations can describe an m^{th} order system in time domain:

$$\begin{aligned} \dot{\bar{x}} &= \bar{\bar{A}}\bar{x} + \bar{B}u \\ y &= \bar{P}^T\bar{x} + Du \end{aligned} \qquad \ldots(1)$$

where u is the input variable, y is the output variable. $\bar{x}$ is the state variable vector and given as

$$\bar{x} = (x_1, x_2, \ldots, x_m)^T . \qquad \ldots(2)$$

Single line over a symbol indicates that the variable is a vector and double line indicates that the variable is a matrix in these equations. A, B, P and D are coefficients and their elements are scalar terms. Although single input-single output system is chosen for simplicity, it is easy to extend the method for multiple input-multiple output system.

Input signal and all state variables must be positive in Eq. (1) and Eq. (2) in order to synthesize a log domain circuit. This situation is explained by Frey[13] and Gilbert[25]. A theorem is proposed by Frey and Tola[24] to solve this issue to design a log domain circuit. In that paper, the systematical state-space representation for differential Class AB filter was presented and it is guaranteed that all devices in the circuit operate in the active region for all circumstances.

According to the theorem mentioned above[24], state variable x and input signal u are splitted into L (Left) and R (Right) sides as shown in Eq. (3) and Eq. (4) as follows:

$$\bar{x} = \bar{x}_L - \bar{x}_R \qquad \ldots(3)$$

$$u = u_L - u_R \qquad \ldots(4)$$

Then splitted state-space variables and input signals are substituted for general state-space representation of Eq. (1) and shown in Eq. (5) and Eq. (6).

$$\begin{aligned} \dot{\bar{x}}_L &= \bar{\bar{A}}_p\bar{x}_L + \bar{\bar{A}}_n\bar{x}_R + \bar{B}_p u_L + \bar{B}_n u_R - \bar{\bar{\psi}}\bar{x}_{LR} \\ \dot{\bar{x}}_R &= \bar{\bar{A}}_p\bar{x}_R + \bar{\bar{A}}_n\bar{x}_L + \bar{B}_p u_R + \bar{B}_n u_L - \bar{\bar{\psi}}\bar{x}_{LR} \end{aligned} \qquad \ldots(5)$$

$$\begin{aligned} y_L &= \bar{P}^T x_L + Du_L \\ y_R &= \bar{P}^T x_R + Du_R \end{aligned} \qquad \ldots(6)$$

where

$$\bar{\bar{A}} = \bar{\bar{A}}_p - \bar{\bar{A}}_n \qquad \ldots(7)$$

$$\bar{B} = \bar{B}_p - \bar{B}_n \qquad \ldots(8)$$

$$\bar{\bar{\psi}} = \begin{pmatrix} \delta_1 & 0 & \cdots & 0 \\ 0 & \delta_2 & \cdots & \vdots \\ \vdots & \vdots & \ddots & \vdots \\ 0 & 0 & \cdots & \delta_m \end{pmatrix} \qquad \ldots(9)$$

$$x_{LR} = [x_{1L}x_{1R}, x_{2L}x_{2R}, \ldots x_{mL}x_{mR}] \quad \ldots(10)$$

The $\overline{\overline{\psi}}$ consists of function $\delta_i(\bar{x}_L, \bar{x}_R, u_L, u_R)$ and it is a diagonal matrix as presented in Eq. (9). This matrix is called as dummy input. These terms are very important for the theorem and they become ineffective when the original signal is obtained[24].

The next step of the realization is mapping of state-space variables and input signal with nonlinear functions. This transformation has to be one-to-one and onto mapping given in Eq. (11) and Eq. (12).

$$\begin{aligned} \bar{x}_R &= \bar{f}(v_R) = [I_s e^{v_{1R}/V_t}, I_s e^{v_{2R}/V_t}, \ldots I_s e^{v_{mR}/V_t}]^T \\ \bar{x}_L &= \bar{f}(v_L) = [I_s e^{v_{1L}/V_t}, I_s e^{v_{2L}/V_t}, \ldots I_s e^{v_{mL}/V_t}]^T \end{aligned} \quad \ldots(11)$$

$$\begin{aligned} u_R &= g(v_{oR}) = I_s e^{v_{oR}/V_t} \\ u_L &= g(v_{oL}) = I_s e^{v_{oL}/V_t} \end{aligned} \quad \ldots(12)$$

Now we consider only *i*th row of the matrix of state-space equations for simplification. Scaling factor $C_i/df(v_i)/dv_i$ is multiplied through the *i*th row, where C_i is constant term. After some manipulations, generalized *m*th order nodal equations are obtained for L and R sides. The equations are given in Eq. (13) and Eq. (14) only for R side due to equations' resemblance.

$$\begin{aligned} C_i \dot{v}_{iR} = {} & \mp I_{fpii} + \sum_{j=1, j\neq i}^{m} I_s \exp\left|(v_{jR} + V_{fpij} - v_{iR})/Vt\right| \\ & + \sum_{j=1}^{m} I_s \exp\left|(v_{jL} + V_{fnij} - v_{iR})/V_t\right| \\ & + I_s \exp\left|(v_{oR} + V_{fopi} - v_{iR})/V_t\right| \\ & + I_s \exp\left|(v_{oL} + V_{foni} - v_{iR})/V_t\right| \\ & - \delta_i I_{fi} I_s \exp\left|v_{iL}/V_t\right| \end{aligned} \quad \ldots(13)$$

$$y_R = I_s \exp\left|v_{1R}/V_t\right| \quad \ldots(14)$$

Where

$$\begin{aligned} I_{fpii} &= V_t C_i A_{pii},\ A_{pii} \geq 0 \\ -I_{fpii} &= V_t C_i A_{pii},\ A_{pii} < 0 \end{aligned} \quad \ldots(15)$$

$$I_{fpij} = V_t C_i A_{pij} = I_s \exp\left|V_{fpij}\right|/Vt,\ i \neq j,\ A_{pij} \geq 0 \quad \ldots(16)$$

$$I_{fnij} = V_t C_i A_{nij} = I_s e\left|V_{fnij}/Vt\right|,\ \mathrm{A_{nij}} \geq 0 \quad \ldots(17)$$

$$\begin{aligned} I_{fopi} &= V_t C_i B_{pi} = I_s \exp\left|V_{fopi}/V_t\right|,\ B_{pi} > 0 \\ I_{foni} &= V_t C_i B_{ni} = I_s \exp\left|V_{foni}/V_t\right|,\ B_{ni} > 0 \end{aligned} \quad \ldots(18)$$

$$I_{fi} = V_t C_i = I_s \exp\left(V_{fi}/V_t\right) \quad \ldots(19)$$

The nodal equations in Eq. (13) and Eq. (14) can be realized by using capacitors, transistors and current sources in log domain.

3. Design

Two integrators, a summer and feedbacks compose the classical KHN structure. The idea of using lossy integrators in KHN structure in log domain is presented in literature[21]. In that work, universal biquad filter was designed by using Class A circuit structure. This work extends the idea for differential Class AB circuit. The designed block diagram is presented in Fig. 1. In the block diagram, y_{LP}, y_{HP}, y_{BP}, y_{AP}, y_N yields to low pass, high pass, band pass, all pass and notch filter outputs, respectively.

$$y_{LP} = \left(\omega_0^2 / \left(s^2 + \frac{\omega_0}{Q}s + \omega_0^2\right)\right)u, \quad \ldots(20)$$

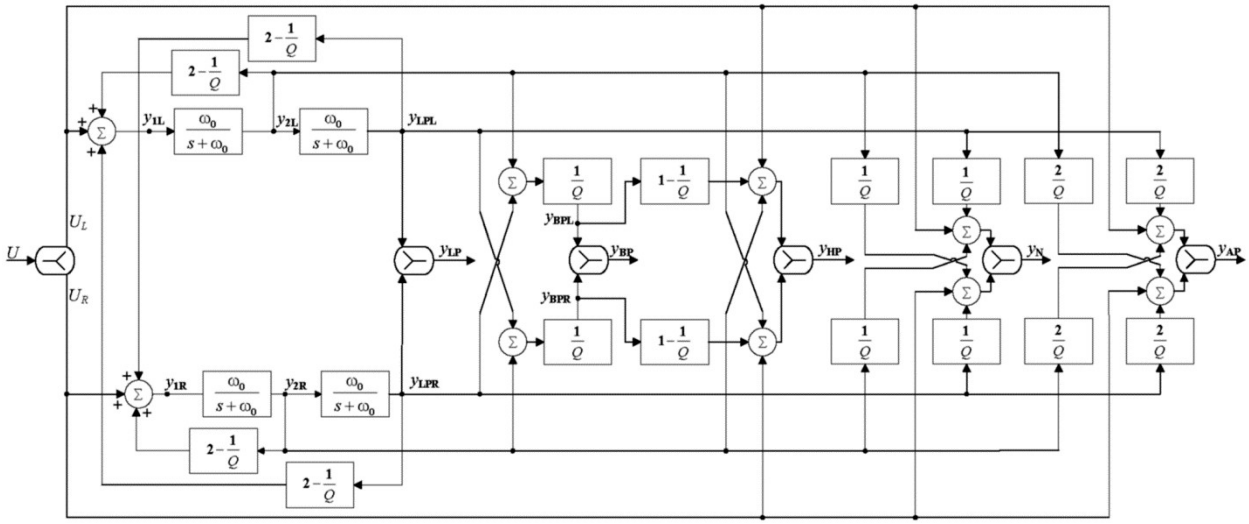

Fig. 1 — Log domain differential Class AB universal filter block diagram.

$$y_{HP} = \left(s^2 / \left(s^2 + \frac{\omega_0}{Q} s + \omega_0^2 \right) \right) u, \quad \ldots(21)$$

$$y_{BP} = \left(\omega_0 s / \left(s^2 + \frac{\omega_0}{Q} s + \omega_0^2 \right) \right) u, \quad \ldots(22)$$

$$y_{AP} = \left(\left(s^2 - \frac{\omega_0}{Q} s + \omega_0^2 \right) / \left(s^2 + \frac{\omega_0}{Q} s + \omega_0^2 \right) \right) u, \quad \ldots(23)$$

$$y_N = \left(\left(s^2 + \omega_0^2 \right) / \left(s^2 + \frac{\omega_0}{Q} s + \omega_0^2 \right) \right) u. \quad \ldots(24)$$

The input signal u must be splitted to two signals namely u_L and u_R which have to be always positive in order to use the signal in differential Class AB circuit structure. This circuit is called current splitter[23] and shown in Fig. 2.

4. Log Domain Differential Class AB Lossy Integrator

To design the Class AB log domain filter circuit shown in Fig. 1, lossy integrator and multiplier blocks must be realized. Realization of current summer block is not needed thanks to current-mode operation.

At first, log domain lossy integrator realization is needed. The lossy integrator circuit is realized by general state-space method for Class AB log domain circuits presented in Section 2. The lossy integrator transfer function is shown below:

$$H(s) = \frac{\omega_0}{s + \omega_0} \quad \ldots(25)$$

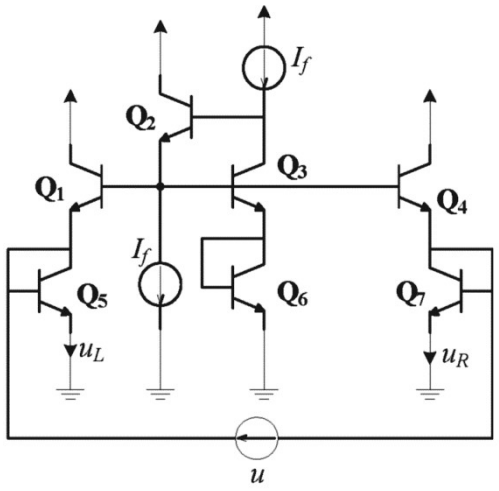

Fig. 2 — Current splitter circuit[23].

where ω_0 is the pole frequency of the lossy integrator.

The state space representations of Eq. (25) are given below:

$$\dot{x} = -\omega_0 x + \omega_0 u \quad \ldots(26)$$

$$y = x \quad \ldots(27)$$

where x is the state variable, u is the input, y is the output. These equations are customized versions of Eq. (3) and Eq. (4):

$$\begin{aligned} u &= u_L - u_R \\ x &= x_L - x_R \\ y &= y_L - y_R \\ \dot{x}_L &= -\omega_0 x_L + \omega_0 u_L \\ y_L &= x_L \end{aligned} \quad \ldots(28)$$

In order to guarantee that the state variable not to be negative, additional term has been added to the equation. This term is not an effective term when the original signal is obtained.

$$\dot{x}_R = -\omega_0 x_R + \omega_0 u_R - m x_L x_R \quad \ldots(29)$$

Eq. (28) and Eq. (29) are related to Eqs (3-6).

If the mapping functions below are applied to the state and input variables like in Eq. (11) and Eq. (12):

$$u_R = I_s \exp\left| v_{0R} / V_t \right| \quad \ldots(30)$$

$$y_R = x_R = I_s \exp\left| v_{iR} / V_t \right| \quad \ldots(31)$$

by using Eq. (29), Eq. (30), Eq. (31) and multiplying with

$$C V_t / I_s \exp\left| v_{iR} / V_t \right| \quad \ldots(32)$$

and we assume that $I_{f1} = I_s \exp|v_{f1}/V_t|$, $I_{f2} = I_s \exp|v_{f2}/V_t|$ then we obtain Eq. (33) and Eq. (34).

$$\begin{aligned} C\dot{v}_{iR} = &-I_{f1} + I_s \exp\left| (V_{f2} + v_{0R} - v_{iR}) / V_t \right| \\ &- I_s \exp\left| v_{iL} / V_t \right| \end{aligned} \quad \ldots(33)$$

$$y_R = I_s e^{v_{iR}/V_t} \quad \ldots(34)$$

where $I_f = \omega_0 C V_t$, and the thermal voltage of the transistor is V_t. Eq. (33) can be written as follows:

$$C\dot{v}_{1R} = -I_f + I_s \exp\left| (v_{0R} + V_f - v_{1R}) / V_t \right| \quad \ldots(35)$$

$$C\dot{v}_{1L} = -I_f + I_s \exp\left| (v_{0L} + V_f - v_{1L}) / V_t \right| \quad \ldots(36)$$

where $V_f = V_t \ln(I_f / I_s)$.

The left side of Eq. (35) looks like as a grounded capacitor's current that is connected to a node which has voltage of v_{1L}. The right side of Eq. (35) can be synthesized by an independent current source and a bipolar transistor which its base is connected to the node that has a voltage of $v_{0R}+V_f$ and its emitter is connected to a node which has a voltage of v_{1R}. Similarly, left side of the lossy integrator circuit could be realized by using Eq. (36). The circuit realized with these considerations is presented in Fig. 3.

5. Current Multiplier

The next process is realizing a multiplier. The circuit is designed by translinear principle[25]. The equation below defines the current multiplier circuit:

$$i_{OUT} = \frac{I_{DC1}}{I_{DC2}} i_{IN} . \qquad \ldots(37)$$

The circuit is shown in Fig. 4. By using the block diagram in Fig. 1, lossy integrator in Fig. 3, current multiplier in Fig. 4 and current mirrors, the whole circuit proposed is shown in Fig. 5.

6. Nonideality

The ideal NPN and PNP bipolar junction transistor models are given in Fig. 6. From here to end of this section, only NPN bipolar junction transistor for nonideal case is presented for simplicity. Same method is also applied to PNP bipolar junction transistor. The following equations can be written for ideal NPN transistor:

$$\begin{aligned} &i_B = 0, \\ &i_C = i_E = i_Q, \qquad \ldots(38) \\ &v_{BE} = v_Q . \end{aligned}$$

The voltage-current relationship for ideal NPN transistor is shown below:

$$i_Q = I_s e^{v_Q / V_t} \Leftrightarrow v_Q = V_t \ln \frac{i_Q}{I_s}. \qquad \ldots(39)$$

Assume that the NPN transistor has finite current gain, β. For this case the new voltage-current relationship is given as:

$$i_E = i_C + i_B = \left(1 + \frac{1}{\beta}\right) I_s e^{v_{BE} / V_t} \qquad \ldots(40)$$

where $\varepsilon = \frac{1}{\beta} i_Q$.

Equation (40) can be written as:

$$\begin{aligned} &i_E = I_s e^{v_Q / V_t} + \frac{1}{\beta} I_s e^{v_Q / V_t}, \qquad \ldots(41) \\ &i_E = i_Q + \varepsilon. \end{aligned}$$

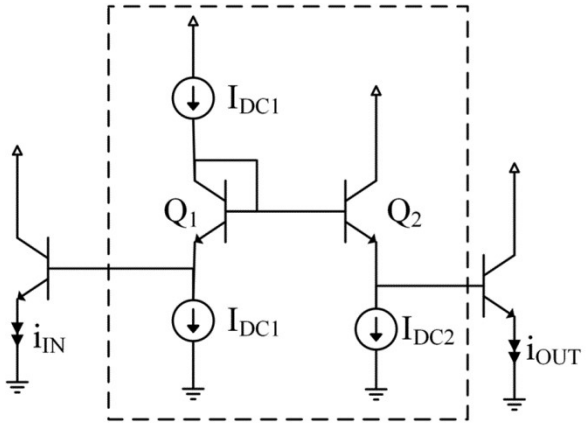

Fig. 4 — Current multiplier circuit.

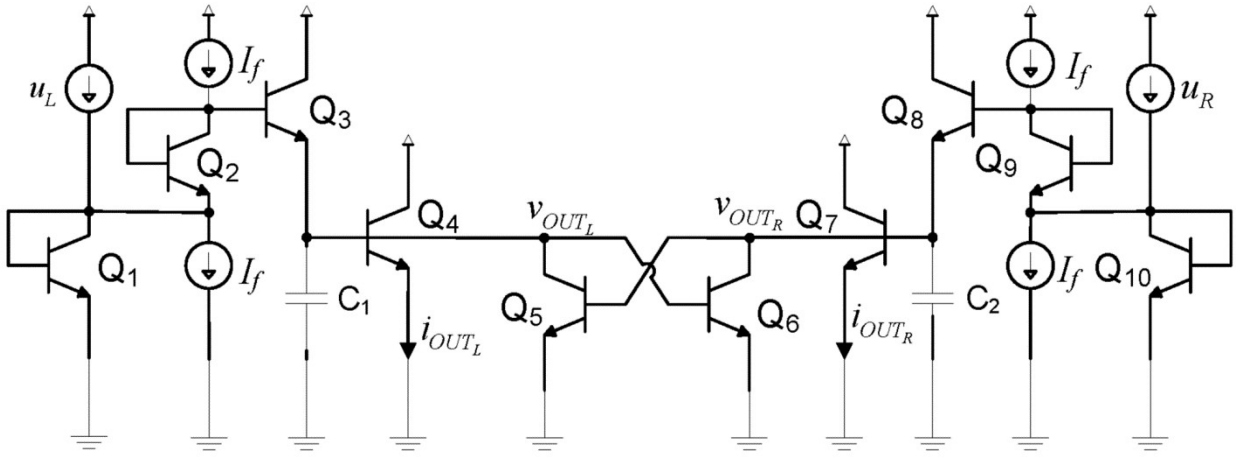

Fig. 3 — Lossy integrator circuit.

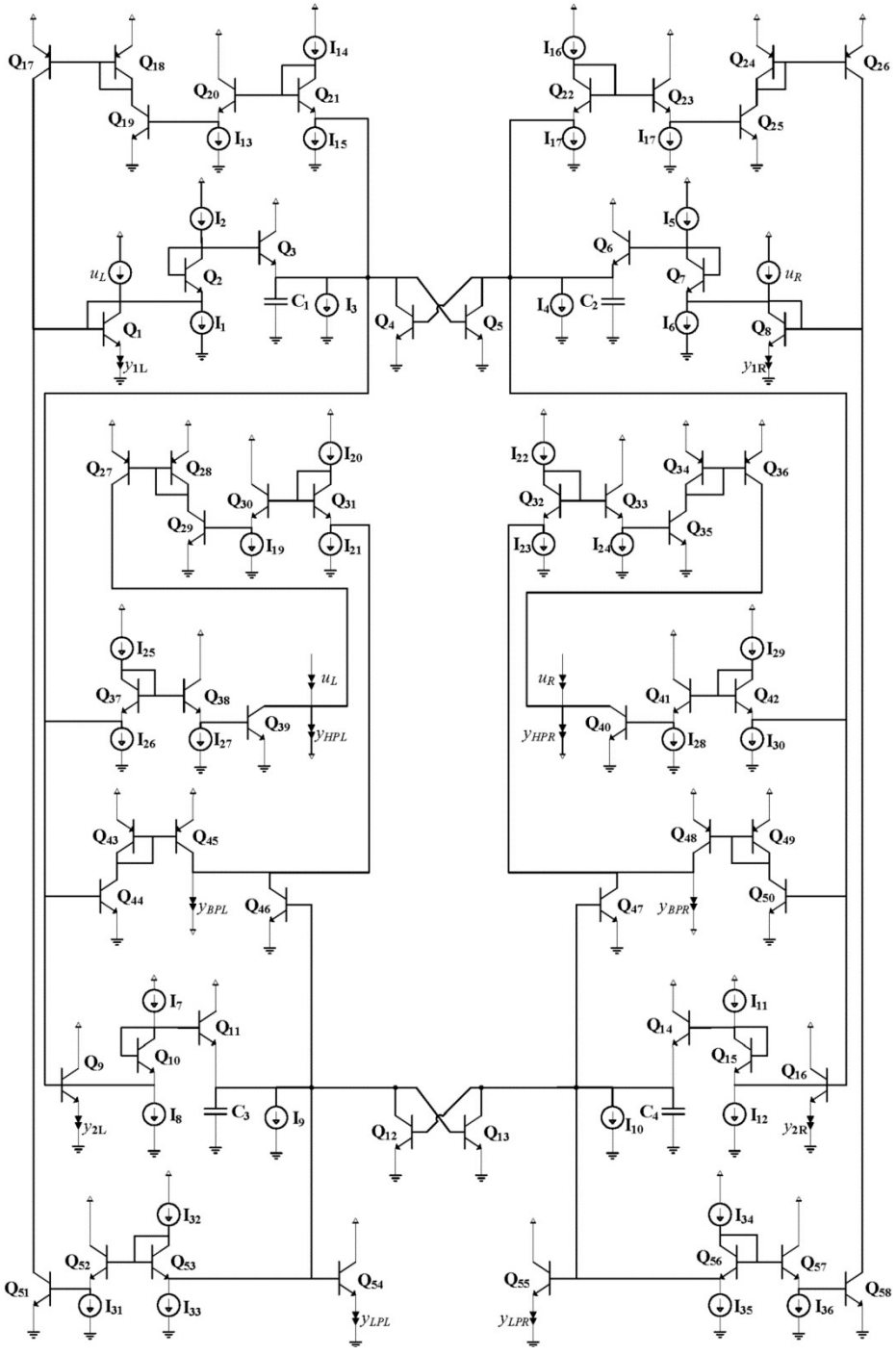

Fig. 5 — Proposed second order universal biquad filter.

The first term of the right side of the Eq. (41) is same as an ideal NPN transistor's voltage-current relation. So that a real NPN transistor's emitter current can be expressed as an ideal NPN transistor's current plus the current that depends on the ideal NPN transistor's current. The new BJT models are presented in Fig. 7[20].

The theoretical method works like this: replace each transistor with the new models in Fig. 7 and calculate the effect to state space equations, after that superpose each effect. Now we have the total effects of non-ideal transistor models to whole circuit[20].

By using the method above we can obtain bipolar junction transistors' nonlinear effects on the

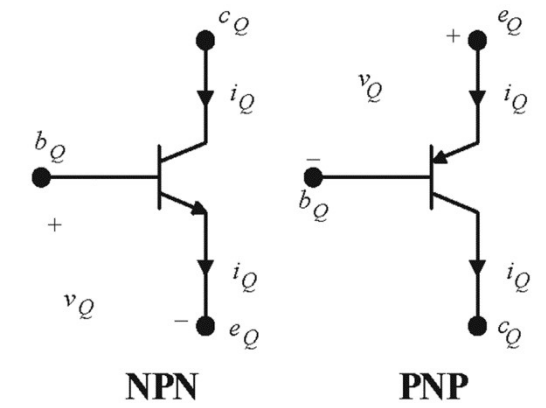

Fig. 6 — The ideal transistor models.

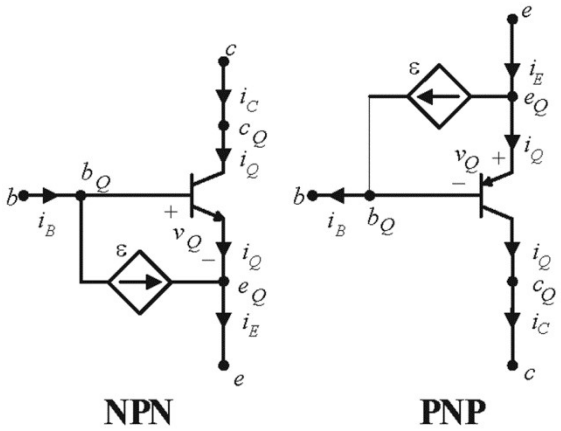

Fig. 7 — The transistor models that have finite current gain [20].

differential class AB lossy integrator circuit shown in Fig. 3. The new state space representation of the lossy integrator circuit with the transistor model that has finite current gain is shown below:

$$\begin{aligned}\dot{x}_L &= -\omega_0 x_R + \omega_0 u_R - m x_L x_R \\ &\quad + \omega_0 u_{d1} + \omega_0 u_{d2} + \omega_0 u_{d3} + \omega_0 u_{d6} \\ \dot{x}_R &= -\omega_0 x_R + \omega_0 u_R - m x_L x_R \\ &\quad + \omega_0 u_{d5} + \omega_0 u_{d8} + \omega_0 u_{d9} + \omega_0 u_{d10} \\ y_L &= x_L + \omega_0 u_{d4} \\ y_R &= x_R + \omega_0 u_{d7}\end{aligned} \quad \ldots(42)$$

where u_{d1} is non-ideal effect of the BJT transistor $Q1$, u_{d2} is non-ideal effect of the BJT transistor $Q2$ and so on.

$$\begin{aligned}&u_{d1} = -\frac{1}{\beta+1}u_L,\ u_{d2} = -\frac{1}{\beta+1}u_L, \\ &u_{d3} = -\frac{\beta I_f u_L}{\beta x_L + I_f + u_L},\ u_{d4} = -\frac{1}{\beta I_f}x_L{}^2, \\ &u_{d6} = -\frac{1}{\beta I_f}x_L{}^2\end{aligned} \quad \ldots(43)$$

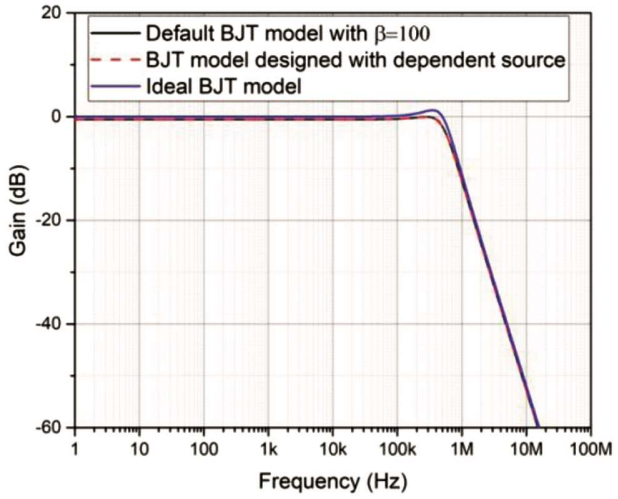

Fig. 8 — Frequency gain response of low pass filter output for investigation of non-ideal BJT effects.

and

$$\begin{aligned}&u_{d5} = -\frac{1}{\beta+1}u_R,\ u_{d7} = -\frac{1}{\beta+1}u_R, \\ &u_{d8} = -\frac{\beta I_f u_R}{\beta x_R + I_f + u_R},\ u_{d9} = -\frac{1}{\beta I_f}x_R{}^2, \\ &u_{d10} = -\frac{1}{\beta I_f}x_R{}^2.\end{aligned} \quad \ldots(44)$$

The additional terms presented above change the transfer function of the differential class AB lossy integrator. These changes in the transfer function expected to be appear in the form of gain loss and difference of the pole frequency of the filter-that is designed by using this lossy integrator-from the theoretically calculated value. PSpice simulations for low pass output of filter circuit in Fig. 5 including current splitter circuit in Fig. 2 are made both default BJT models with β=100 and with the models presented in Fig. 7 to verify the method. Frequency gain response presented in Fig. 8, frequency phase response in Fig. 9 and transient response in Fig. 10 prove that the method is valid and changes in the transfer function appear in the form of gain loss and difference of the pole frequency of the low pass filter output.

7. Simulation Results

At first, the synthesized filter circuit simulations in PSpice are performed using ideal transistors which are default bipolar transistor models that have BF=10000. The PSpice simulation results verified the theoretical results. Input current u is sinusoidal. The voltage

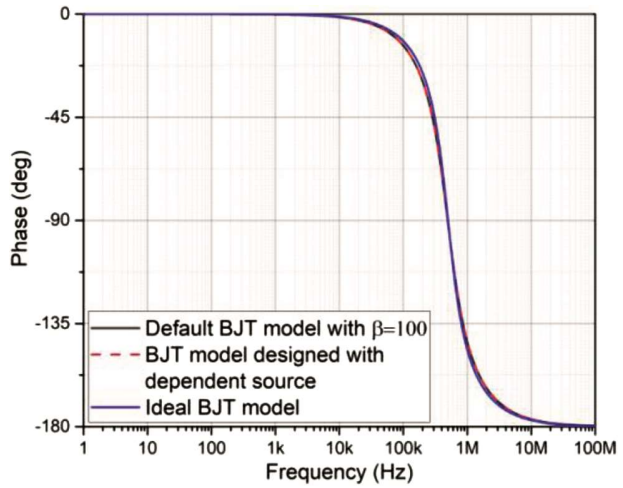

Fig. 9 — Frequency phase response of low pass filter output for investigation of non-ideal BJT effects.

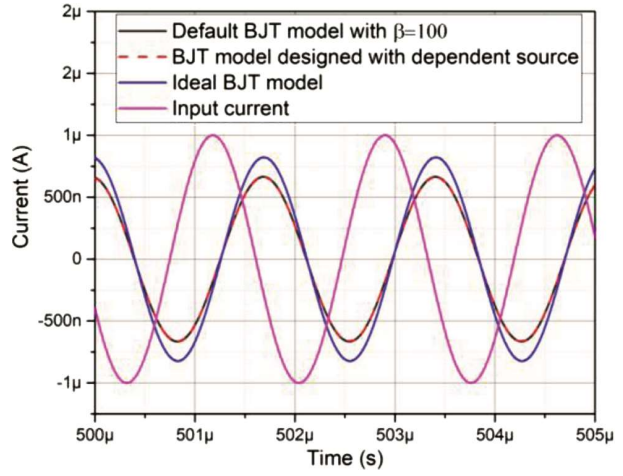

Fig. 10 — Transient response of low pass filter output for investigation of non-ideal BJT effects.

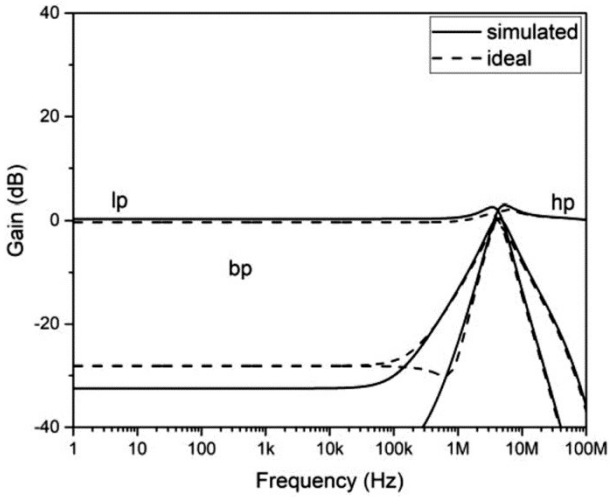

Fig. 11 — Fundamental filters' frequency-gain responses.

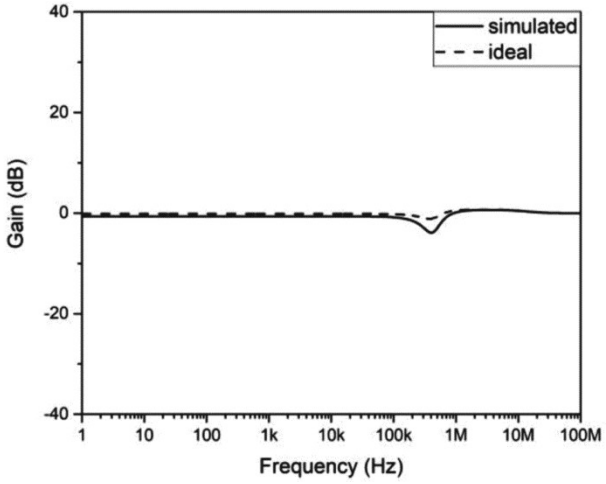

Fig. 12 — The gain frequency response of all pass filter.

source is 2.25 V. Capacitances of lossy integrators are chosen to be C_1=C_2=C_3=C_4=123 pF. The amplitudes of current sources I_1-I_{13}, I_{18}, I_{19}, I_{24}-I_{31}, I_{36} are set to be I_f ; I_{14}-I_{17}, I_{32}-I_{35} are set to be (2-1/Q)I_f ; I_{20}-I_{23} are set to be (1-1/Q)I_f where I_f =10 μA. The pole frequency obtained from PSpice simulations with these values is f_0=501.187 kHz, the calculated value of pole frequency is f_0=500 kHz where I_f=$\omega_0 C V_t$.

The simulation results verified the theoretical works, so the next step is using real transistor models in simulations. AT&T CBIC-R type real transistor models have nonlinear characteristics that caused the current gain characteristics of some blocks in Fig. 1 are less than the theoretically calculated values. In order to solve this issue, some transistors' area values and some current sources' amplitudes are slightly changed.

To obtain AC response of the circuit that has quality factor Q=1 and calculated pole frequency of f_0=500 kHz, PSpice simulations are performed. The frequency-gain responses of low pass, high pass and band pass filters' are given in Fig. 11. In the figure, the simulation results both performed by using ideal transistor models and real transistor models are coherent with each other. All pass filter's frequency-gain and frequency-phase responses are presented in Figs 12 and 13. Notch filter's frequency-gain and frequency-phase responses are presented in Figs 14 and 15. The quality factor and the pole frequency of the filter are tunable by changing values of the DC current sources. These are advantages of this circuit that the designer can use the filter for wide frequency range without any component replacement. In Fig. 16, the pole frequency f_0 is swept two decades by varying

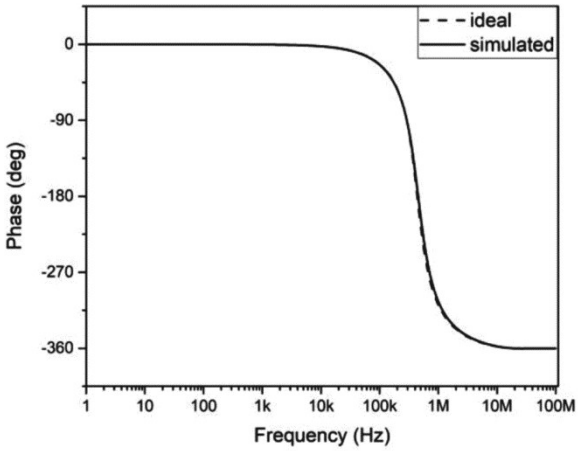

Fig. 13 — The phase frequency response of all pass filter.

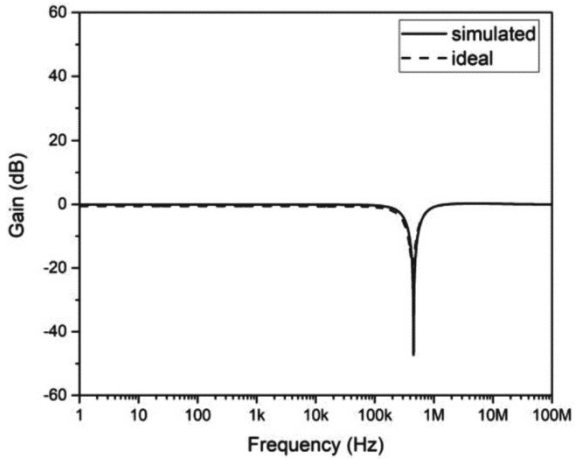

Fig. 14 — The gain frequency response of notch filter.

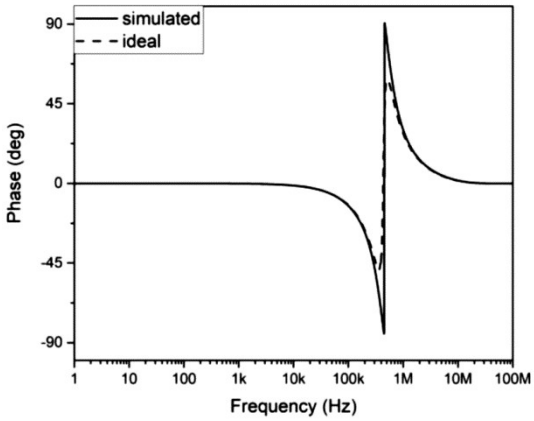

Fig. 15 — The phase frequency response of notch filter.

the amplitudes of current sources which I_f is set to 1 µA for f_0=47.206 kHz, I_f is set to 10 µA for f_0=465.586 kHz, I_f is set to 100 µA for f_0=4.305 MHz where the amplitude of the input signal's sinusoidal part is set to $0.1I_f$. Electronic tunability of quality factor is shown in Fig. 17 which Q is set to 5.

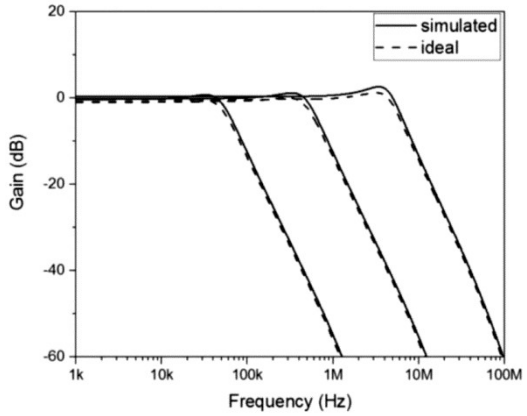

Fig. 16 — Tunable pole frequency f_0 for low pass filter.

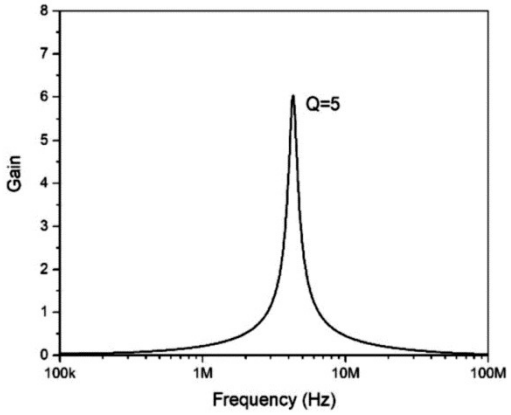

Fig. 17 — Band pass filter gain response for Q=5.

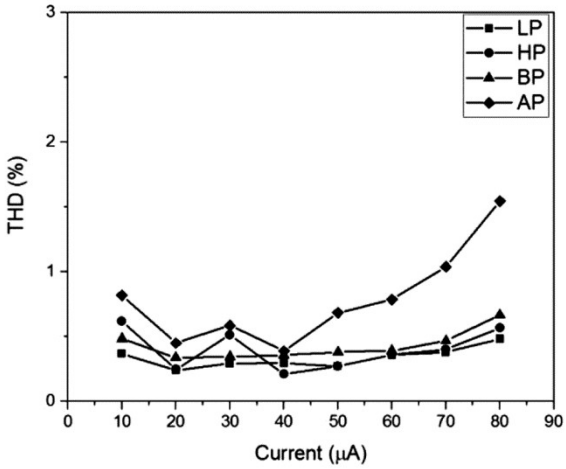

Fig. 18 — THD values.

Output signal's THD was measured for some values of input current for all filter responses except notch filter. The results are shown in Fig. 18. DC current I_f is set to 100 µA, sinusoidal input signal u is swept from 10 µA to 80 µA.

8. Conclusions

A new log domain differential class AB filter is realized which has low pass, high pass, band pass, all pass and notch filter outputs in this study. It is the first time that lossy integrators are deployed to realize log domain differential Class AB filter. Lossy integrator circuit and current multiplier circuit have been designed to synthesize the universal filter. Lossy integrator circuit is designed by using state space synthesis method and translinear circuit theory.

Current multiplier circuit is designed by using translinear circuit theory. The quality factor Q and the pole frequency f_0 of the filter are electronically tunable by only adjusting amplitudes of the DC current sources.

Non-ideal effects of bipolar junction transistors are investigated by modelling finite current gain characteristics of BJTs. In PSpice simulations, the effects are appeared as gain loss and difference in the pole frequency from the calculated values of low pass filter. That was expected in mathematical calculations obtained from the BJT models that have finite current gain.

The PSpice simulations are performed with both ideal and real transistor models that are AT&T CBIC-R type. The simulation results of the circuit obtained from PSpice verified the theoretical results. Frequency domain and time domain simulation results prove that the quality factor Q and the pole frequency f_0 of the filter are electronically tunable.

Acknowledgment

This work is based on work supported by Scientific Research Projects Coordination Unit of Pamukkale University, under Project number of 2015FBE027.

References

1 Kerwin W J, Huelsman L P & Newcomb R W, *IEEE J Solid-State Circuits*, 2 (1967) 87.
2 Sedra A S & Smith K C, *Microelectronic circuits*, (Oxford University Press: New York), 6th Edn, (2009) 1254.
3 Salama K N & Soliman A M, *Frequenz*, 54 (2000) 90.
4 Ibrahim M A & Kuntman H, *AEU - Int J Electron Commun*, 58 (2004) 429.
5 Sedra A S & Smith K C, *IEEE Trans Circuit Theory*, 17 (1970) 132.
6 Soliman A M, *Electron Lett*, 30 (1994) 2019.
7 Senani R & Singh V K, *Electron Lett*, 31 (1995) 626.
8 Toker A, Özoğuz S & Acar C, *Electron Lett*, 35 (1999) 1682.
9 Altuntaş E & Toker A, *AEU - Int J Electron Commun*, 56 (2002) 45.
10 Ibrahim M A, Minaei S & Kuntman H, *AEU - Int J Electron Commun*, 59 (2005) 311.
11 Keskin A Ü, Biolek D, Hancioglu E & Biolkova V, *AEU - Int J Electron Commun*, 60 (2006) 443.
12 Tola A T, Arslanalp R & Yilmaz S S, *AEU - Int J Electron Commun*, 63 (2009) 600.
13 Frey D R, *Circuits, Devices Syst IEE Proc G*, 140 (1993) 406.
14 Frey D R & Steigerwald L, *IEEE Int Symp Circuits Syst*, 96 (1996).
15 Frey D R, *IEEE Trans Circuits Syst I Fundam Theory Appl*, 43 (1996) 34.
16 Punzenberger M & Enz C, *Log-domain filters for low-voltage low-power applications*. IEEE International Conference on Electronics, Circuits and Systems, 1998.
17 Tsividis Y P, *IEEE Trans Circuits Syst II Analog Digit Signal Process*, 44 (1997) 65.
18 Tsividis Y P, Gopinathan V & Toth L, *Electron Lett*, 26 (1990) 1331.
19 Seevinck E, *Electron Lett*, 26 (1990) 2046.
20 Tola A T, A *study of nonideal log domain and differential class AB filters*, Ph D Thesis, Lehigh University, 1999.
21 Duduk N & Tola A T, *Elektron ir Elektrotechnika*, 22 (2016) 56.
22 Duduk N & Tola A T, *A study about effects of transistors' nonideal characteristics on log domain filters*. Applied Electronics (AE), 2012 International Conference, Plzen, 2012.
23 Tola A T & Frey D R, *Anal Integr Circuits Signal Process*, 550 (2000) 57.
24 Frey D R & Tola A T, *IEEE Trans Circuits Syst II: Anal Digital Signal Process*, 46 (1999) 306.
25 Gilbert B, *Electron Lett*, 11 (1975) 14.